



Cultivar, site or harvest date: the gordian knot of wine terroir

L. M. Schmidtke¹ · G. Antalick^{1,2} · K. Šuklje^{1,3} · J. W. Blackman¹ · J. Boccard⁴ · A. Deloire^{1,5}

Received: 17 July 2019 / Accepted: 30 March 2020
© Springer Science+Business Media, LLC, part of Springer Nature 2020

Abstract

Introduction The complex interactions of vine cultivars, and localised regional climate associated with specific vineyard sites are important attributes to the concept of terroir and significant contributors to grape maturity and wine sensory profiles. An improved understanding of the influence of each factor and their interactions is a challenging conundrum, and will enable more efficient production targeting specific wine styles.

Objectives To characterise the metabolic flux of grape berries and resulting wines to characterise the relative impact of site specific climate, cultivar, and grape maturity based upon berry sugar accumulation models that consistently target specific wine styles.

Methods A spatial and temporal study of grape and wine composition was undertaken for two important cultivars in two distinct regions of New South Wales. Measures of composition and wine sensory ratings were simultaneously analysed using a multiblock algorithm taking advantage of the ANOVA framework to identify important contributions to wine style arising from grape maturity, vineyard site and cultivar.

Results A consistent flux of grape and wine constituents is evident for wine made from sequentially harvested grapes from the same vineyard with increasing levels of grape maturity. Contributions of region and vineyard site to wine style could also be elucidated. Differences in metabolite flux in grapes and resulting wines between cultivars growing in similar conditions are evident.

Conclusions The combination of a metabolomics and multiblock data decomposition approach may be successfully used to profile and elucidate the contribution of abiotic factors to grape and wine composition and provide improved understanding of the terroir concept.

Keywords Viticulture · Oenology · AMOPLS · Grapes · Climate · Shiraz · Cabernet sauvignon

Electronic supplementary material The online version of this article (<https://doi.org/10.1007/s11306-020-01673-3>) contains supplementary material, which is available to authorized users.

✉ L. M. Schmidtke
lschmidtke@csu.edu.au

¹ School of Agricultural and Wine Sciences, National Wine and Grape Industry Centre, Charles Sturt University, Locked Bag 588, Wagga Wagga, NSW 2678, Australia

² Present Address: Wine Research Centre, Univerza v Novi Gorici, Vipavska 13, 5000 Nova Gorica, Slovenia

³ Present Address: Department of Fruit Growing, Viticulture and Oenology, Agricultural Institute of Slovenia, Hacquetova 17, 1000 Ljubljana, Slovenia

⁴ Institute of Pharmaceutical Sciences of Western Switzerland, University of Geneva, Rue Michel-Servet 1, 1211 Geneva 4, Switzerland

⁵ Present Address: L'Institut Agro (SupAgro), 2 Place P. Viala, 34060 Montpellier, France

1 Introduction

The association of agricultural products to a provenance or specific region (terroir) that imparts typical sensorial qualities is an important concept for providers of high value products. Increasing consumer demand and interest for foods and wines associated with, and which identify with specific regions and places of production, are important economic and marketing factors for product differentiation and uniqueness (Charters et al. 2017). The concept of a terroir is complex and is broadly considered in terms of the interactions between the environment, climate and the social interplay of people, their history and traditional approaches to food production (Seguin 1986). In the wine and food industries several definitions of terroir exist and all acknowledge the importance of a local climate upon the composition of grapes, resulting wines or foods (Gladstones 2011). Viticultural management,

including varying grape maturity at harvest, and wine making practises will also significantly alter the final wine styles (Matthews 2015). Wine style depends principally on grape composition which is largely determined by abiotic factors and vineyard's environmental characteristics. Differences in grape composition pertaining to site arise from vines adapting to different biotic and abiotic environments (Tonietto and Carbonneau 2004) which in turn influence vine physiology and ultimately berry composition (Deloire et al. 2008). Single markers that define wine style, terroir or regionality are simplistic and identification of an array of markers is required to determine objective and predictive wine sensory features (Schmidtke et al. 2013). Determining the impact of specific drivers of terroir is a challenging analytical task requiring robust experimental design, careful site selection, longitudinal studies and application of sophisticated data driven algorithms to tease out vineyard, vintage and abiotic factors associated with wine style and typicality. Untargeted metabolomic approaches characterising the volatile or non-volatile signatures of grapes (Anesi et al. 2015; Cramer et al. 2014); and wine components (Roullier-Gall et al. 2014) have suggested some measures of terroir. However, very few studies have characterised the relative contributions and importance of aspects of terroir being site, cultivar, mesoclimate and grape maturity to wine style. Mesoclimate is especially interesting in the context of terroir and refers to the scale of climate influenced by local geographies and landscapes within hundreds of metres to several kilometres according to altitude and topography, and is therefore an important consideration to vineyard site selection (Carbonneau et al. 2015). In this investigation we report on a designed experiment, with targeted measures of grape and wine composition, to characterise the influence of multiple vineyard sites in two distinct wine regions of Australia (Orange and Griffith). This allowed the investigation of different growing conditions, and grape maturity at harvest, on grape and resulting wine composition and sensory domains for two important cultivars (*Vitis Vinifera* cv. Shiraz and Cabernet Sauvignon). One region is warm (Griffith), characterised by a flat topography with little variation between sites and mesoclimate, whereas the second region (Orange) is characterised by variable vineyard elevation enabling inferences on the influence of climate associated with cooler growing conditions. Using a data-driven multiblock approach within a multivariate Analysis of Variance framework that exploits balanced experimental designs, the influences of grape maturity, cultivar and mesoclimate at vineyard site on the resulting wine chemical and sensory domains is demonstrated.

2 Data analysis using analysis of variance multiblock orthogonal partial least squares (AMOPLS)

Multiple analytical techniques are often used to determine sample composition resulting in contemporaneous data sets that characterise specific attributes. For example GCMS and LCMS, or other analytical techniques, may be used to measure the volatile and non-volatile composition of grape and wine samples made when vines are exposed to several treatments (Šuklje et al. 2016). Classic experimental designs that make use of Analysis of Variance (ANOVA) partitioning of data variation, enable the combined effect of several experimental factors (EF) upon sample composition to be determined. In the present study, an ANOVA multiblock orthogonal partial least squares (AMOPLS) approach, first described by Boccard and Rudaz (2016) was used to analyse multiple data sets pertaining to the composition of grapes, wines and their sensory features to determine the impact of factors associated to the concept of terroir. A general outline of the AMOPLS approach is shown in Supplementary Fig. 1 representing an experiment with n samples and several data blocks with k_i variables. All data must be collated and organised such that sample order in each data block is identical. The first part of the AMOPLS approach (Supplementary Fig. 1, panel A (1)) consists of block scaling and concatenation. Each centred data block is normalized for variance to ensure equal contributions to the overall model. Once each data block is scaled, a data superblock ($n \times \sum k_i$) is created by horizontal concatenation of all data blocks (Supplementary Fig. 1, panel A (2)). The second part of the AMOPLS data decomposition (Supplementary Fig. 2, panel B (3)) is to partition sources of variation according to an ANOVA model of explanatory factors which creates a series of equally sized data tables ($n \times \sum k_i$) by computing the mean values of all measurements for each level of the explanatory factor. Once an explanatory factor data table has been determined, it is subtracted from the experimental matrix prior to computation of the next explanatory factor table, thus each table is additive and orthogonal and represents the experimental design structure summarising the explanatory factor main effects and interactions according to the general linear model equation:

$$X = X_{\mu} + X_{\alpha} + X_{\beta} + X_{\alpha\beta} + X_{res} \quad (1)$$

where X_{μ} is the overall mean value for each variable, X_{α} , X_{β} and $X_{\alpha\beta}$ contain the mean values for each level of the explanatory factors α , β and their interaction $\alpha\beta$, and residuals represented by X_{res} respectively. The residual data table therefore contains the measured variable responses that are unable to be related to a known explanatory factor of the

experimental design, and may be stochastic or systematic and unrelated to the overall experimental design.

The directions of variations in the data within each data table representing the explanatory factors α, β and thier interaction $\alpha\beta$, is used to create a response matrix (Y). The response matrix is created by extracting the non-zero eigenvectors following a singular value decomposition of each of the explanatory factor data tables (Supplementary Fig. 1, panel B (4)). Thus an estimation of the barycentre of each orthogonal explanatory factor level is derived in vector form, and these are collated into a response matrix (Y) for supervised data modelling.

Prior to data decomposition the residual matrix is added back to each of the explanatory factors data tables (Supplementary Fig. 1, panel B (5)). Thus each specific data table contains variation associated with the explanatory factors levels α, β or interaction $\alpha\beta$, along with the residuals which represents a common source of variation. This approach is analogous to the data matrices constructed for several multivariate ANOVA based approaches for data analysis (Bouveresse et al. 2011; Harrington et al. 2005; Jansen et al. 2005). An OPLS regression (Rantalainen et al. 2007) is then used to predict the response matrix (Y) from the residual augmented explanatory factor data matrices which can be represented using the following equations (Supplementary Fig. 1, panel B (6)):

$$X = T_{p\alpha}P_{pa}^T + T_{p\beta}P_{p\beta}^T + T_{p\alpha\beta}P_{p\alpha\beta}^T + T_oP_o^T + E \tag{2}$$

$$Y = T_{p\alpha}Q_{p\alpha}^T + T_{p\beta}Q_{p\beta}^T + T_{p\alpha\beta}Q_{p\alpha\beta}^T + F \tag{3}$$

where X is the experimental data matrix comprising of Y -predictive and orthogonal latent variables. Each Y -predictive component is intrinsically linked to the ANOVA explanatory factors used to construct the designed experiment. With this approach matrices of scores and loadings for each ANOVA explanatory factor, and interaction terms can be derived from the multiblock data. Thus Y -predictive scores $T_{p\alpha}, T_{p\beta}$ and $T_{p\alpha\beta}$, and loadings $P_{p\alpha}, P_{p\beta}$ and $P_{p\alpha\beta}$ for factors α, β and the interaction term $\alpha\beta$ are obtained. Orthogonal scores (T_o) and loadings (P_o) associated with the residual matrix X_{res} and E represent the residual matrix of the AMOPLS model for X . The response matrix is estimated from all predictive scores ($T_{p\alpha}, T_{p\beta}$ and $T_{p\alpha\beta}$) and corresponding predictive loadings for each Y -response ($Q_{p\alpha}, Q_{p\beta}$ and $Q_{p\alpha\beta}$) with F representing the AMOPLS residual matrix for Y .

The OPLS component of the AMOPLS model is determined using a multiple kernel approach that commences with determining association matrices for each residual augmented data table derived from ANOVA variance partitioning (Supplementary Fig. 1, panel C (7)).

An association matrix (W_1 to W_i : where i represents the number of explanatory factor data tables for the ANOVA model) is computed from the XX^T scalar product. Each association matrix has the same squared dimensions being equal to the number of observations or rows. A global consensus matrix (W_G) derived from the summed association matrices (Supplementary Fig. 1, panel C (8)) is used as the X matrix in the dual form of the OPLS (Supplementary Fig. 1, panel C (9)) according to Eqs. (2) and (3).

Permutation testing of the Y response matrix within each explanatory factor (1000 iterations), is used to determine the optimum number of extracted orthogonal components for the overall model and the number of predictive components is equal to the number of responses in the Y matrix. Model quality is assessed by overall model goodness of fit (R^2Y) and a residual structure ratio (RSR) that reflects the reliability of each main effect or interaction by computing a ratio of contribution between a given effect and the residuals. The RSR is therefore determined from latent structures and offers complementary measures of experimental levels effects, thus when model R^2Y and RSR values are significant, interpretive information can be extracted from the predictive model components.

A noteworthy feature of the AMOPLS approach is the ability to determine the relative contributions of each data block to the overall model (Supplementary Fig. 1, panel C (10)). This can be determined since each Y response is orthogonal so each predictive component is therefore focused on a single explanatory factor, and linearity for data deflation and modelling is maintained. Data block weights or saliences for a specific component are determined from the corresponding predictive scores and association matrix in accordance with the following equation:

$$\lambda_i = t^T W_i t_d \tag{4}$$

where λ is the block salience for each significant component, t is a vector of predictive scores and W_i is the XX^T product kernel matrix for each specific data block.

The interpretation of the AMOPLS results is then performed like any latent variable model, based on scores describing the distribution of the samples and loadings associated with variables coefficients to build the components. Additional information is offered by the AMOPLS model by calculating: (i) the salience of each effect to a component and (ii) the contribution of each of the data blocks to this component. Therefore, each direction of variation associated with a component can be objectively associated to a specific effect and its construction can be explained based on the contributions of the blocks. By these means, signal variations can be decomposed according to both the experimental design and the structure of the data collection.

3 Materials and methods

3.1 Vineyard sites

Vitis vinifera cv. Shiraz and Cabernet Sauvignon (CS) were sampled from commercial vineyards in the Griffith and Orange regions during the 2013–14 and 2014–15 growing seasons. The Griffith region is characterised by a flat topography with altitude differences between vineyards (designated G1, G2, G3 and G4) of 12 m and distance between vineyards is approximately 15 km. Vineyards in Orange were from two distinct sites; O1 was 650 m above sea level (asl) whereas second vineyard, O2, was 870 m asl, and the distance between them was around 25 km. Weather stations were installed 2 m above ground level to measure mesoclimatic data, soil moisture loggers installed and stem water potential measurements (SWP) were performed regularly during the season. Drilled climatic data obtained from SILO (Queensland, Australia) were used to calculate typical viticultural indices that describe the climate of regions/vineyards. Due to the flat Griffith terrain and no observed differences in mesoclimatic data (not shown) between the monitored vineyards, climatic indices were calculated for one location only, and considered representative for all vineyards for this region for the present investigation. Huglin and Cold night index were calculated from 1949/50 to 2015/16 season (Tonietto and Carbonneau 2004). Climatic indices were calculated separately for O1 and O2 with long term climatic data are presented in Supplementary Table 1 and the principal features of the vineyards and cultivation summarised in Supplementary Table 2.

3.2 Vineyard monitoring of grape maturation and link to potential wine style

Grape harvesting targeted berry maturation stages corresponding to ‘fresh’, ‘intermediate’ and ‘mature’ (designated H1, H2 and H3 respectively) based upon a proposed model of potential wine styles according to sugar accumulation profiles (Deloire 2013) as illustrated in Supplementary Fig. 2. The vineyards were monitored weekly from veraison to identify berry sugar accumulation profiles from a population of berries (data not shown). Harvest dates did not deviate from this model by more than 3 days for each vintage. For Shiraz, harvest occurred post sugar accumulation plateau at; 12 days for H1, 18 days for H2 and 24 days for H3. Due to the longer ripening period for CS, harvest occurred at 20, 32 and 40 days for H1, H2 and H3 respectively. Prior to grape harvesting for wine production, vineyards were randomly sampled weekly prior to

veraison by collecting ten representative bunches in triplicate per site until sugar concentration reached 18–22 Brix whereupon samples were collected every 3 days. Grape berries (100/replicate) were excised with the pedicel to avoid juice loss, weighed and crushed for measurements of juice total soluble solids (TSS) content, and calculation of sugar accumulation per berry (mg/berry) to determine the point of a plateau of berry sugar accumulation (Shahood et al. 2019).

3.3 Grape berry sampling and analysis

Grape berry samples (100 berries/replicate, in triplicate) were randomly collected from grape clusters across each experimental block evenly from both sides of the canopy, and from top, middle and bottom of bunches (Supplementary Fig. 3), immediately frozen in liquid nitrogen and stored at -80°C until analysis. A random subsample of 50 frozen berries from each replicate were deseeded using mortar and pestle, pooled and ground to a fine powder with IKA A11 basic analytical mill (IKA, Malaysia). Grape powder was stored at -80°C until further analyses.

Grape juice samples (in triplicate) were collected from freshly harvested grapes for winemaking after crushing and basic parameters analysed using standard techniques (Iland et al. 2004). Grape yeast assimilable nitrogen (YAN) comprising α -amino acids and ammonia in juice were measured by enzymatic tests (Thermo Fisher, Sydney) and calculated from ammonium and free amino nitrogen (FAN) measurements.

Grape berry powder was analysed for organic acids and carbohydrate content whereas wines were analysed for residual sugar content by HPLC according to previously published methods (Frayne 1986). Briefly, two 300 mm \times 7.8 mm Aminex HPX-87H ion exclusion columns and micro guard column (Bio-Rad, Berkeley, USA) at 65°C interfaced to a Waters 600 controller (Milford, USA), Waters 717 plus autosampler, Waters photodiode array (PDA) and refractive index (RI) detectors. Grape berry powder was prepared according to published methods (Eyéghé-Bickong et al. 2012) and filtered through a 0.45 μm filter (Merck, Frenchs Forest, Australia) prior to analysis; wine samples were filtered (0.45 μm) and analysed directly.

Grape amino acids were extracted from frozen powder using published methods (Gika et al. 2012) with some modifications; 100 ± 0.05 mg of grape berry powder was weighed into a 1.5 mL Eppendorf tube and extracted with 0.1 mL of 80:20 MeOH:MilliQ (v:v) in an ultrasonic bath for 15 min. Samples were centrifuged (Beckman Coulter, Microfuge 20 Series, Brea, USA) at 13,000 rpm for 10.5 min, the supernatant collected, diluted 1:24 (v/v) with 0.25 M borate buffer (pH 8.5) containing l-hydroxyproline (13.1 mg/L) as internal standard, derivatised with 9-fluorenylmethyl chloroformate

and analysed as described (Haynes et al. 1991). Grape berry anthocyanins were analysed using described methods (Downey and Rochfort 2008) with quantification at 500 nm expressed as malvidin-3-O-glucoside equivalents. Briefly, a precise quantity (100 mg) of homogenised grape powder was weighed into a round bottom 2 mL Eppendorf tube and extracted for 20 min in an ultrasonic bath in 1 mL 50:50 Methanol:MilliQ water. Extracts were analysed by Waters Acquity ultrahigh pressure liquid chromatograph (UPLC) equipped with photodiode array detector (DAD). Mobile phases consisted of aqueous A 10% formic acid in MilliQ water and B 10% formic acid in methanol. A linear gradient with a flow of 0.4 mL/min was employed as follows: 0–1.5 min from 10 to 12% B; 1.5–6.0 min 22% B; 6.0–8.0 min 25% B; 8.0–9.5 min 35% B; 9.5–10.0 100% B, 10.5–13.0 min 100% B, 13.5–14.0 min 10% B and column equilibration with initial conditions to 15.5 min.

Grape carotenoids were extracted from 1 g frozen grape berry powder samples according to (Wehrens et al. 2013) and analysed according to (Young et al. 2016). Briefly, dried carotenoid extract was re-dissolved in 100 µL of ethyl acetate. A 50 µL aliquot was mixed with 200 µL methanol (Lashbrooke et al. 2010) and directly injected onto a Waters Acquity UPLC equipped with UPLC BEH Shield RP18 (2.1 mm × 100 mm, 1.7 µm) protected with a Waters UPLC BEH guard cartridge (2.1 mm × 100 mm, 1.7 µm) and DAD detector. Carotenoids were quantified at 450 nm, whereas chlorophylls and pheophytin were quantified at 660 nm.

Total grape volatiles, terpenes and norisoprenoids were determined using described methods (Šuklje et al. 2016). Sample preparation was carried out according to the methods of (Loscos et al. 2009) and (Young et al. 2016). Briefly, 0.5 g of grape berry sample was weighed into a 20 mL glass vial followed immediately by 2 mL of tartrate buffer in concentration 5 g/L of tartaric acid and 3 g/L ascorbic acid, pH 3, sodium chloride (1 g) was added to the vial which was sealed using a screw cap with Teflon liner and heated at 100 °C for an hour. Thereafter vials were cooled and injected into the GCMS with conditions as described in Šuklje et al. (2016). Semi quantitative data were normalised on a sample weight and internal standard response.

Sample preparation for free grape volatiles (C6 compounds, norisoprenoids and terpenes) was carried out according to published protocols (Matarese et al. 2014). Briefly, 2 g of frozen grape berry powder was weighed into cooled SPME vial. To the frozen sample, 2 mL of phosphate-citrate buffer (0.1 M Na₂HPO₄ and 50 mM citric acid, pH 5) was added followed by 10 µL of ascorbic acid at concentration 200 g/L. Samples were thereafter spiked with 15 µL of internal standard mix as described above for total volatile analysis. Sodium chloride (1 g) was added to the vial which was immediately capped, vortexed and analysed. Analytical sample sequences did not exceed 12 samples

with randomised sample order. Samples were analysed by head space solid-phase micro extraction (HS-SPME) with a PDMS-CAR-DVB 50/30 µm fibre (Supelco, Bellefonte, USA). Volatiles absorbed by the fibre were released into an Agilent 7890 gas chromatography equipped with a DB-WAXetr capillary column (60 m, 0.25 mm, 0.25 µm film thickness, J&W Scientific, Folsom, CA) and coupled with a Gerstel MPX autosampler with a Peltier tray cooler set at +4 °C. The GC was connected to a 5975C mass spectrometer (Agilent Technologies) as described in Šuklje et al. (2016). Semi quantitative data were normalised on a sample weight and internal standard response.

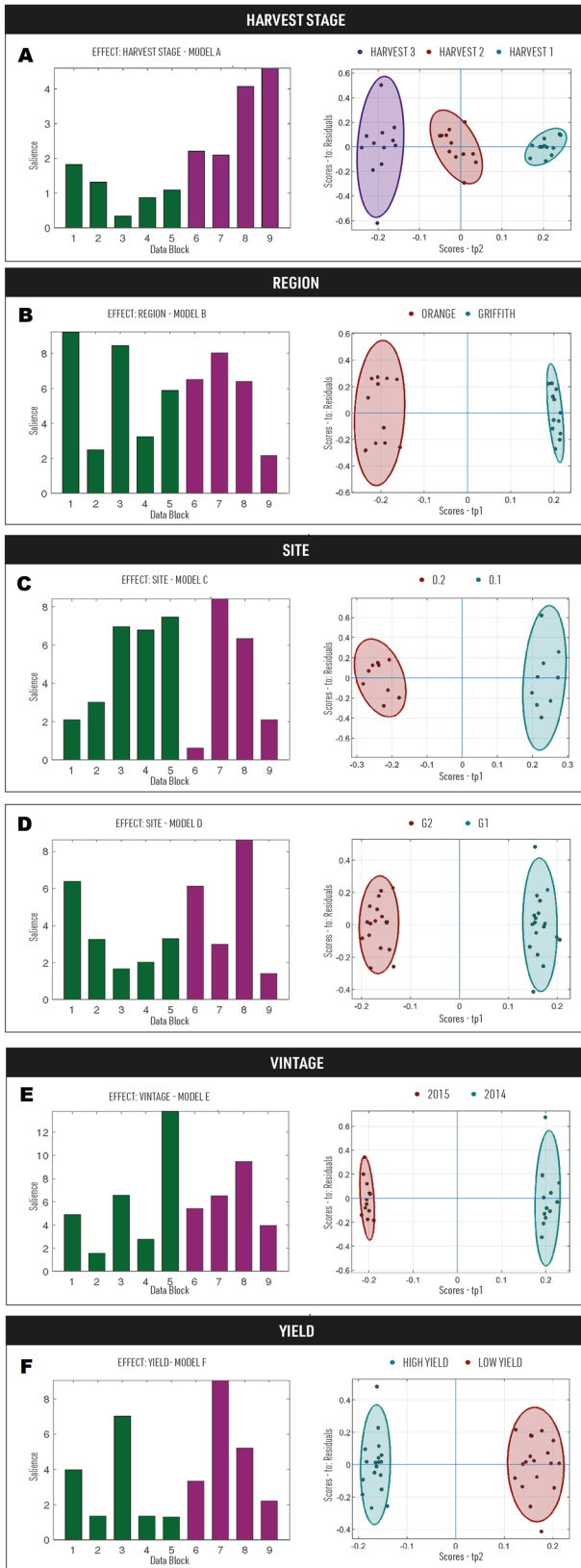
3.4 Winemaking

To minimise vine variability within each vineyard plot, grapes (3 × 60 kg replicates) were randomly harvested for winemaking across the experimental site picking only a few bunches per vine using a similar approach for grape sampling (Supplementary Fig. 3). Vinifications were performed as described (Šuklje et al. 2019). All biological replicates were kept separate during grape processing. Grapes were destemmed, crushed and transferred to 100 L stainless steel tanks for fermentation. Acidity was adjusted to approximately pH 3.6 with tartaric acid. The must was inoculated with *Sacharomyces cerevisiae* yeast EC1118 (Lalvin) and fermentations were carried out at 25–26 °C. For ferments with an initial TSS of less than 23.4 Brix, once alcoholic fermentation had caused a decrease of 2 to 3 Baumé, the original YAN was adjusted to 200 mg/L with Fermaid K (Lallemant, Australia) and diamonium phosphate. For ferments in excess of 23.4 Brix, the YAN was adjusted to 220 mg/L. Malolactic fermentation was carried out by co-inoculation of *Oenococcus oeni* Enoferm alpha (Lallemant) 2 days after the start of alcoholic fermentation. Wines were pressed off the skins with a small basket press to a pressure of 1 bar when residual sugar level dropped below 0.5 g/L. Pressed wines were placed at 22 °C until the competition of malolactic fermentation and thereafter sulfured with 80 mg/L of sulfur dioxide, pH adjusted to pH 3.6 and racked from lees. Wines were cold stabilised for 21 days at +4 °C, free sulfur dioxide was adjusted to 30 mg/L and bottled prior to sensory analysis.

3.5 Targeted analysis of wine composition

Wine total anthocyanins, colour parameters and polyphenols were analysed as previously described (Iland et al. 2004) with samples adjusted to pH 3.5 and measurements conducted using a UV-1700 Shimadzu spectrophotometer (Kyoto, Japan). Wine total tannins were analysed by methyl cellulose precipitation tannin (Sarneckis et al.

Cultivar: Shiraz



Cultivar: Cabernet Sauvignon

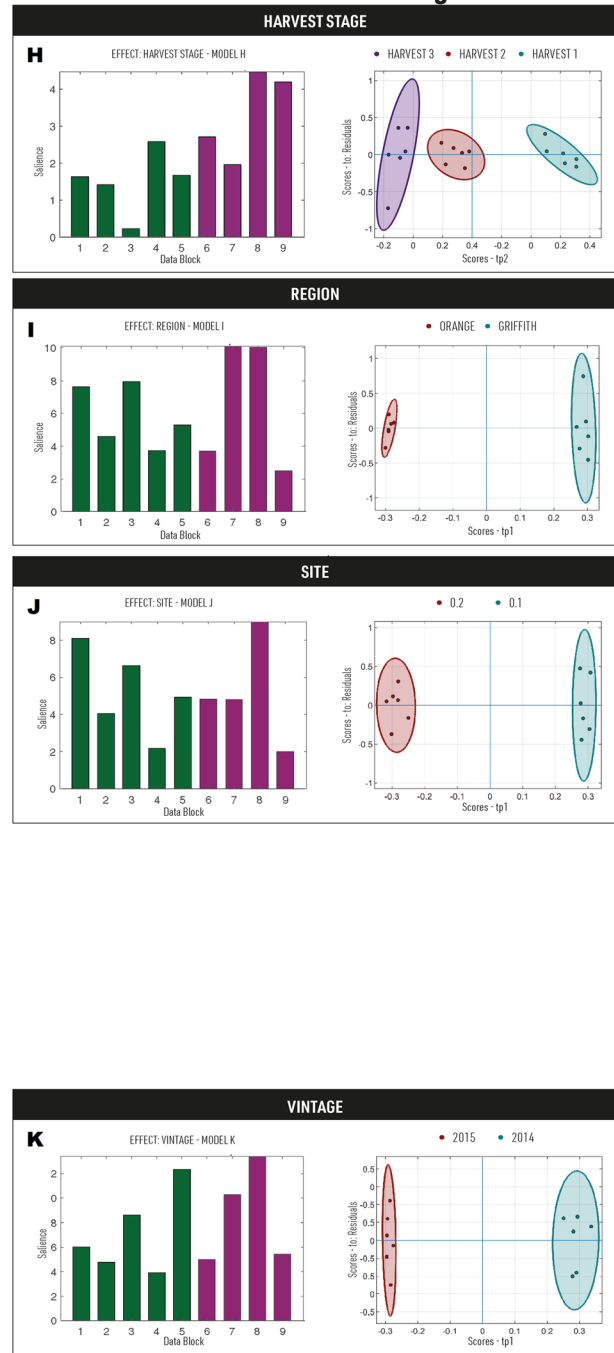


Fig. 1 Data block salience and sample groupings for explanatory factors harvest stage, region, site, vintage and yield for Shiraz and Cabernet Sauvignon cultivars. Saliency values for each data block indicate the relative contribution of that data block to sample clusters in the AMOPLS model. Green bars in the saliency plot refer to grape composition with purple representing wine associated parameters. Ellipses represent the 95% confidence intervals based on Hotelling T^2 values. Block 1: Grape amino acids; Block 2: Grape carbohydrates and organic acids; Block 3: Grape anthocyanins; Block 4: Grape carotenoids; Block 5: Grape volatile compounds; Block 6: Wine making parameters; Block 7: Wine chemistry; Block 8: Wine volatile compounds; Block 9: Wine sensory descriptive analysis

2006) and expressed as epicatechin equivalents. Ethanol was measured with an Anton Paar Alcolyser with DMA 4500 density meter (Graz, Austria).

Wine esters, higher alcohols, C6 compounds and lactones, were analysed according to published methods (Antalick et al. 2010, 2015; Šuklje et al. 2016). Briefly, a mixture of isotopically labelled esters from CDN isotopes (Pointe-Chaire, Canada) was used to quantify esters and higher alcohols (semi-quantification) whereas octan-2-ol (Fluka, Castle Hill, Australia) was used as internal standard for C6 and lactone compounds. Samples were spiked with the internal standard solution mixed containing 20 mg/L [$^2\text{H}_5$]-ethyl butyrate, 20 mg/L [$^2\text{H}_5$]-ethyl hexanoate, [$^2\text{H}_{15}$]-ethyl octanoate, 4 mg/L [$^2\text{H}_{23}$]-ethyl decanoate, 5 mg/L [$^2\text{H}_5$]-ethyl cinnamate and 5 mg/L 2-octanol. In this study, 5 mL wine sample was added to a 20 mL SPME vial with 3 g sodium chloride and 5 mL deionized water, and spiked with 10 μL of internal standard solution. Vials were immediately capped, vortexed, and analysed by head space solid-phase micro extraction with a PDMS-CAR-DVB fibre. Wine volatiles were analysed on the same equipment as detailed for grape volatiles.

3.6 Descriptive sensory analyses of wines

Descriptive sensory analyses (DA) were conducted six months post bottling using published methods (Blackman and Saliba 2009). Twelve experienced panellists (6m, 6f) generated, refined and compiled the final attributes and descriptors (Supplementary Table 3). Panellists were trained to consistently detect, identify and rank the selected aroma and mouth feel attributes, and formal assessment of the wines was conducted over three sessions, in individual tasting booths using red lighting to prevent colour bias. Attributes were ranked using a 9-point line scale anchored from 'absent' to 'high intensity'. For the purposes of whole of systems metabolomics data analysis the mean sensory rating for each wine replicate and sensory attribute were determined from all panellist scores.

3.7 Statistical analyses

ANOVA multiblock orthogonal PLS (AMOPLS) (Boccard and Rudaz 2016), which makes use of balanced sample data sets to investigate the effects of multiple experimental factors within an ANOVA framework, was employed for data analysis.

Analytical values for grape and wine samples were arranged into data matrices according to sample analysis (Table 1) for each cultivar. Combinations of samples to create balanced models for EF (*site, harvest stage, vintage, yield, region*) were selected from the total sample pool is presented in Table 2 with Shiraz and Cabernet Sauvignon cultivars modelled separately. Sample combinations for each model were selected to create a balance design with consideration of vineyard and cultivar parameters (Supplementary Table 2) which are known to influence grape composition irrespective of the EF. For instance, grapevine yield is highly dependent on vine management practices unrelated to climate, limiting the inclusion of sites G3 and G4 to EF yield models. The importance of each EF and interactions, along with the factor levels in discriminating samples can be determined from confidence intervals (95%) of sample scores based upon Hotelling T^2 criteria. Sample scores plots for each factor plotted against the sample scores for the residual matrix are presented in Fig. 1. To assess the consistency of the influence of measured variables for significant EF in multiple AMOPLS model, variable loadings associated with EF that were significant for Shiraz and Cabernet Sauvignon models (Table 3) were used for hierarchical cluster analysis (HCA) using Euclidean distance measures and Wards grouping criteria (Supplementary Figs. 4 and 5). Prior to HCA, model scores and loadings were rotated to ensure consistency in presentation of factor levels in scores plots for each model, and variable standardisation applied. A conservative interpretation of the HCA heat maps was considered appropriate and a summary heat map for each explanatory factor and measured attribute, based upon the mean loading value for variables within the EF of interest, is presented in Fig. 2. Variables are organised with regard to data blocks and colour coded with regard to relative change for harvest stage and region for both Shiraz and Cabernet Sauvignon; and vineyard site within similar or different mesoclimates for Shiraz, with shading indicating the 25th, 50th and 75th percentile values (interquartile range) for the up and down regulation based upon loading amplitude for identical EF from all models. All data analysis was conducted using Matlab (Version: 9.2.0.556344 (R2017a), The Mathworks, Natick); HCA was conducted using the clustergram function supplied with the Bioinformatics toolbox (version 4.8.2017a). Source code for AMOPLS models and permutation testing is available from <https://gitlab.unige.ch/Julien.Boccard/amopls>.

Table 1 Data block descriptions and numbers of measured variables for each sample used in a metabolomics approach to data analysis

Data block		Number of measured features	
		Shiraz	Cabernet sauvignon
1	Grape amino acids	14	14
2	Grape carbohydrates and organic acids	5	5
3	Grape anthocyanins	8	8
4	Grape carotenoids	9	9
5	Grape volatile compounds	28	28
6	Wine making parameters	9	9
7	Wine chemistry	14	14
8	Wine volatile compounds	45	46
9	Wine sensory descriptive analysis	11	13

Differences in the number of sensory attributes and volatile compounds for Shiraz and Cabernet Sauvignon reflect the importance of some attributes associated with certain cultivars

4 Results and discussion

4.1 General climatic differences of vineyards

The median Huglin index calculated for Griffith for the 1949/50 to 2016/17 seasons was 2809, classifying the region as warm. Griffith has temperate night temperatures, with an average minimum of 16.3 °C between January and March. According to the same long-term data, the Orange

O1 and O2 vineyards have median Huglin indexes of 2337 and 1971, which classifies them as temperate-warm and temperate respectively. The cold night indexes were 14.2 and 12.6 °C for O1 and O2 respectively, corresponding to temperate to cool nights (Tonietto and Carbonneau 2004).

The 2013/14 and 2014/15 growing seasons were warmer than long-term median values. Calculated Huglin indices were 3140, 2621 and 2234 for Griffith, O1 and O2 respectively in the 2014/15 season and 3028, 2505 and 2137 in season 2013/14. In the seasons investigated, Griffith was a classed as very warm, O1 was warm, and O2 was temperate-warm (Tonietto and Carbonneau 2004). Despite the slightly higher Huglin indexes in 2014/15 season, the cold night index was lower, indicating milder ripening conditions. This was particularly obvious in Orange, where the cold night index was 0.8 °C and 1.0 °C lower in O1 and O2 compared to the figures from the 2013/14 vintage.

4.2 Multivariate models of terroir and grape maturity

Climate is recognised to be one of the most important drivers of grapevine gene expression, grape composition and therefore wine sensory features (Santo et al. 2018). In this investigation we have attempted to identify aspects of terroir by partitioning variances associated with specific EF (*Harvest Stage, Region, Site, Yield and Vintage*) that influence wine features using a longitudinal study of samples from commercial vineyards in two wine regions. Loadings for each significant EF contributor for Shiraz and Cabernet Sauvignon are presented as heat maps in supplementary Figs. 4 and 5. Groupings of similar EF loadings are evident

Table 2 Shiraz and Cabernet Sauvignon grape, wine and sensory explanatory factors and levels for balanced AMOPLS analysis. Varying colours represent explanatory factor levels for each AMOPLS model

Cultivar	Levels	Explanatory Factors														n		
		Site				Harvest Stage			Vintage		Yield		Region					
		G1	G2	G3	G4	O1	O2	H1	H2	H3	V14	V15	High	Low	G		O	
Shiraz	A	■	■			■	■	■	■	■								36
Shiraz	B					■	■	■	■							■	■	24
Shiraz	C					■	■	■	■									18
Shiraz	D	■	■					■	■	■								18
Shiraz	E	■	■					■	■	■	■	■	■					24
Shiraz	F	■	■	■	■			■	■	■				■	■			36
Shiraz	G	■	■					■	■	■								12
Cab. sauvignon	H							■	■	■	■	■	■					12
Cab. sauvignon	I							■	■	■						■	■	18
Cab. sauvignon	J					■	■											12
Cab. sauvignon	K							■	■	■	■	■	■					12
Cab. sauvignon	L							■	■	■						■	■	12

Table 3 Metabolomic models performance data

Model	Explanatory factor	Relative sum of squares (%)	RSS p value	RSR	RSR p value
Shiraz					
A	Site	54.4	0.001	11.90	0.001
	Harvest stage	10.7	0.001	3.54	0.001
	Site	12.4	0.951	1.69	0.024
	Residuals	22.5	NA	1.00	1
B	Region	32.3	0.001	2.32	0.001
	Harvest stage	13.4	0.001	1.03	0.289
	Region × harvest stage	4.1	0.446	1.02	0.534
	Residuals	50.2	NA	1.00	1
C	Site	31.2	0.001	4.75	0.001
	Harvest stage	23.3	0.001	2.80	0.001
	Site × harvest stage	11.7	0.455	1.17	0.289
	Residuals	33.7	NA	1.00	1
D	Site	31.1	0.001	5.78	0.001
	Harvest stage	22.8	0.001	3.16	0.001
	Site × harvest stage	13.5	0.26	1.57	0.024
	Residuals	32.7	NA	1.00	1
E	Vintage	33.8	0.001	7.74	0.001
	Harvest stage	9.3	0.001	2.22	0.001
	Site	18.3	0.001	4.26	0.001
	Vintage × Site	8.2	0.073	1.95	0.001
	Vintage × harvest stage	7.5	0.103	1.77	0.001
	Site × harvest stage	2.1	0.905	1.02	0.537
	Residuals	20.9	NA	1.00	1
F	Site	17.9	0.001	5.00	0.001
	Yield	14.4	0.001	3.27	0.001
	Harvest stage	17.1	0.001	4.77	0.001
	Site × yield	5.9	0.409	1.25	0.028
	Site × harvest stage	11.7	0.002	3.39	0.001
	Harvest stage × yield	3.9	0.867	1.11	0.182
	Residuals	29.1	NA	1.00	1
G	Site	33.7	0.003	4.31	0.001
	Harvest stage	26.8	0.003	3.41	0.001
	Site × harvest stage	7.6	0.546	1.07	0.404
	Residuals	31.8	NA	1.00	1
Cabernet Sauvignon					
H	Vintage	62.0	0.006	13.04	0.001
	Harvest stage	9.6	0.007	2.21	0.001
	Vintage × harvest stage	6.3	0.607	1.45	0.093
	Residuals	22.2	NA	1.00	1
I	Region	52.0	0.001	12.97	0.001
	Harvest stage	18.6	0.001	3.83	0.001
	Region × harvest stage	7.7	0.728	1.31	0.163
	Residuals	21.7	NA	1.00	1
J	Site	42.5	0.003	5.82	0.001
	Harvest stage	14.3	0.004	2.11	0.001
	Site × harvest stage	11.3	0.198	1.63	0.042
	Residuals	31.9	NA	1.00	1
K	Vintage	44.4	0.008	5.34	0.001
	Harvest stage	21.1	0.006	2.58	0.001

Table 3 (continued)

Model	Explanatory factor	Relative sum of squares (%)	RSS p value	RSR	RSR p value
L	Vintage × harvest stage	7.5	0.549	1.00	0.851
	Residuals	27.0	NA	1.00	1
	Region	50.8	0.009	8.99	0.001
	Harvest stage	19.2	0.003	3.51	0.001
	Region × harvest stage	6.2	0.650	1.33	0.104
	Residuals	23.8	NA	1.00	1

Relative sums of squares for effects, RSR indices and associated p-values for each effect
p values indicated in bold are considered significant ($p < 5\%$)

suggesting consistent expression of traits for the models, and to assist in the interpretation of measured attributes a summary heat map is presented in Fig. 2.

As expected, vintage was the predominant explanatory factor for grape and wine composition accounting for up to 62% of variation in modelled data for Cabernet Sauvignon and 33% for Shiraz, when this explanatory factor was modelled across sites and harvest dates (Table 3). The high contribution of vintage to compositional models is well supported by previous studies (Anesi et al. 2015). It appears to be region specific as indicated by the diametric positions of vintage for Orange and Griffith in the HCA for Cabernet Sauvignon (Supplementary Table 4), inferring a close associated with mesoclimate and cultivar. Whilst vintage is a dominant factor for grape and wine composition, the terroir concepts of regional and site specific factors that consistently influence wine style attributes are of greater interest for this study. A single model only for the yield EF was evaluated for Shiraz which constrains interpretation to more general inferences from the model loadings presented in the Supplementary Fig. 4. Yield modified grape and wine composition as shown by the two clusters observed on the representation of yield (Fig. 1) with around 14% of data variance partitioned to this EF. Whilst yield and vintage are important contributors to grape and wine composition in this study, the contribution of cultivar, vineyard site and fruit maturity are more interesting and novel findings and therefore these will be considered in detail.

4.2.1 Harvest maturity (H1, H2 and H3)

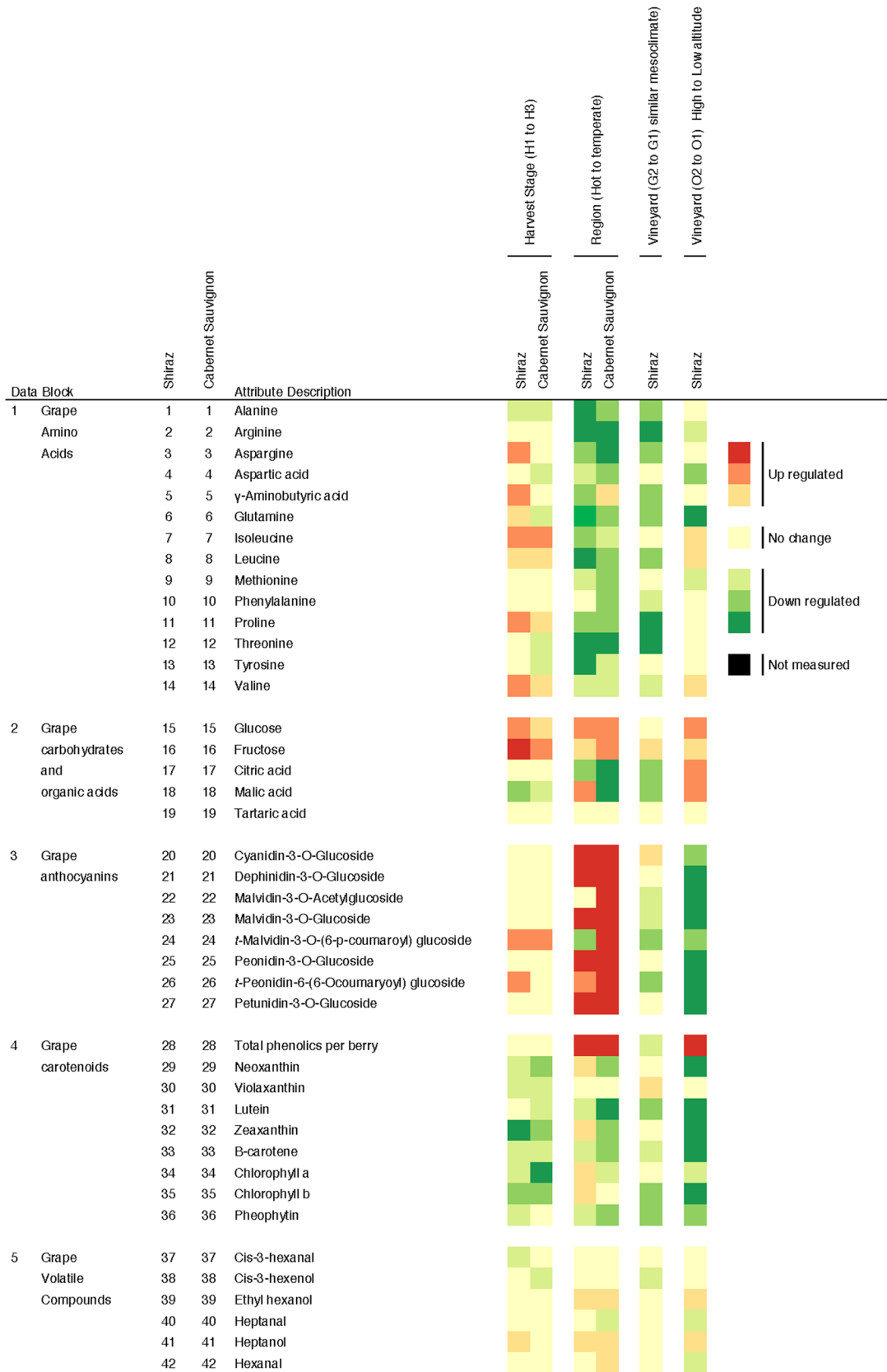
All models for both cultivars show a common clustering of samples according to the explanatory factor grape maturity at harvest (EF: *Harvest H1, H2 & H3*) with clearly separate sample groups regardless of vintage, region or site (Fig. 1, model A & H) accounting for between 9 and 27% of total data variance (Table 3). These results show that sensory spaces corresponding to H1 (fresh fruit), H2 (intermediate) and H3 (mature fruit) stages were associated to specific

Fig. 2 Aggregated heat map data for important Experimental Factors associated with grape cultivar, grape maturity at harvest, region vineyard and altitude. Attribute numbers for Shiraz and Cabernet Sauvignon correspond to the heat maps in the supplementary figures. Cultivar specific changes are displayed for the measured attributes arranged in data blocks used for AMOPLS. For harvest stage relative changes in expression are apparent with increasing grape maturation (H1 to H3). For region relative changes are apparent when vineyard locations change from hot to temperate mesoclimate. For vineyards in a similar mesoclimate, changes are evident which reflect specific vineyard management intervention. For comparison of vineyards with different altitude from high to low elevation, changes in attribute expression largely reflects progression to higher temperatures for vine growth

grape or wine compositions irrespective of vintage growing conditions.

Salience values for EF *Harvest* show a similar pattern of data block contributions to the sample groupings for both cultivars (Fig. 1, models A & H) and is influenced mostly by wine volatile composition (block 8) and wine sensory aspects (block 9), followed by wine making parameters (block 6), and wine chemistry (block 7) for Shiraz; and grape carotenoids (block 4) for CS, indicating a progression of berry and wine attributes common to both cultivars. While grape and juice composition might contribute to characterise fresh, intermediate and mature stages, it seems that wine volatiles and sensory profiles were the most influential factors, discriminating grape maturity stages at harvest, which largely reflects the empirical sensory evidence used to establish the ripening models (Deloire 2013). Of the remaining data blocks, grape berry amino acid composition (block 1) has a modest contribution reflecting the importance of the amino acid profile in wine volatile compound profiles and therefore wine sensory scores. Differences in amino acids with harvest timing for Shiraz is evident and more apparent than for Cabernet Sauvignon, which reflects the increased sensitivity of Shiraz to abiotic stress (Hochberg et al. 2015).

Attributes in grapes (block 2) including berry glucose and fructose continued to increase during the maturation period up to harvest, primarily due to berry weight loss in late ripening possibly through transpiration and xylem back



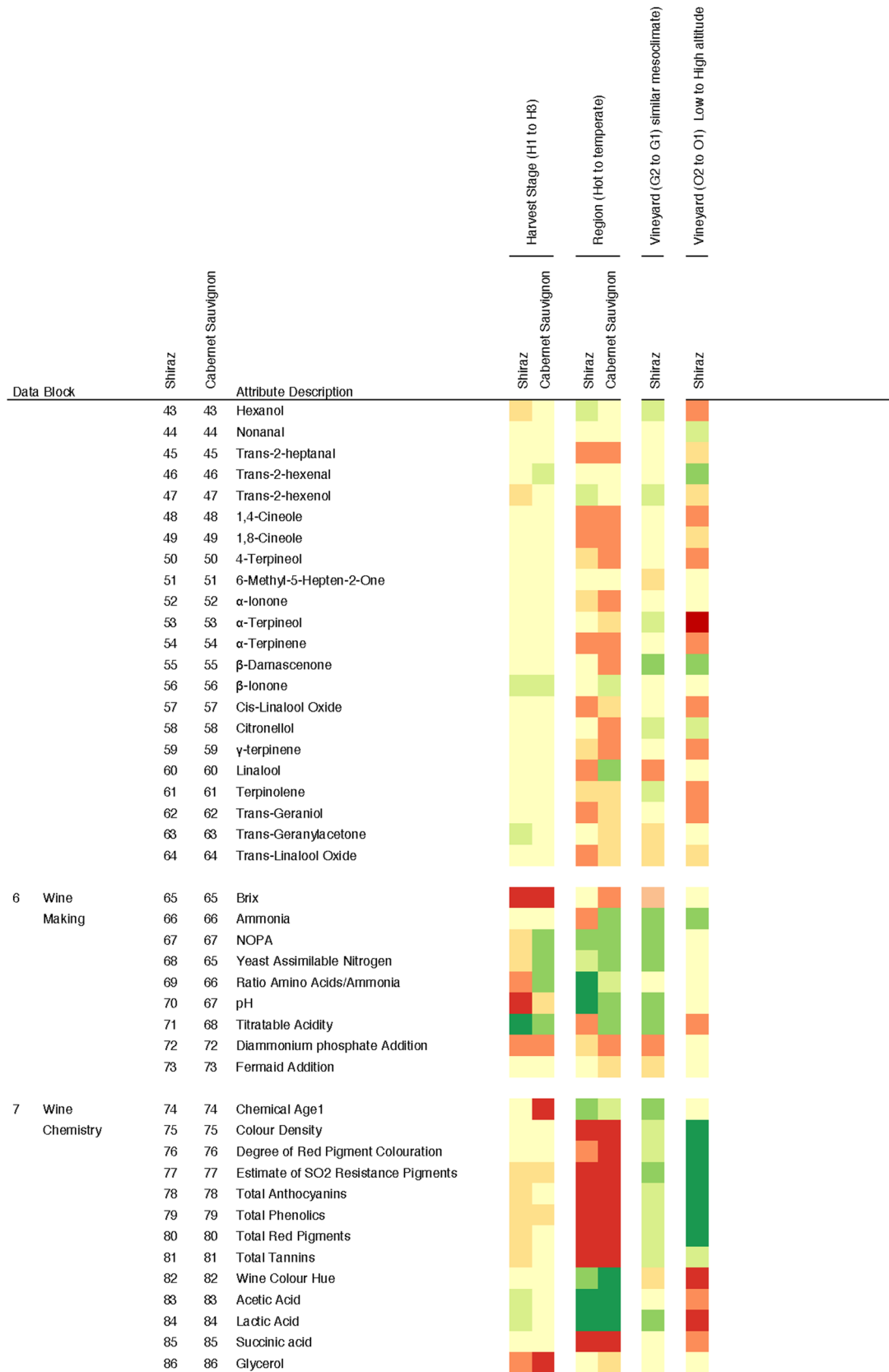


Fig. 2 (continued)

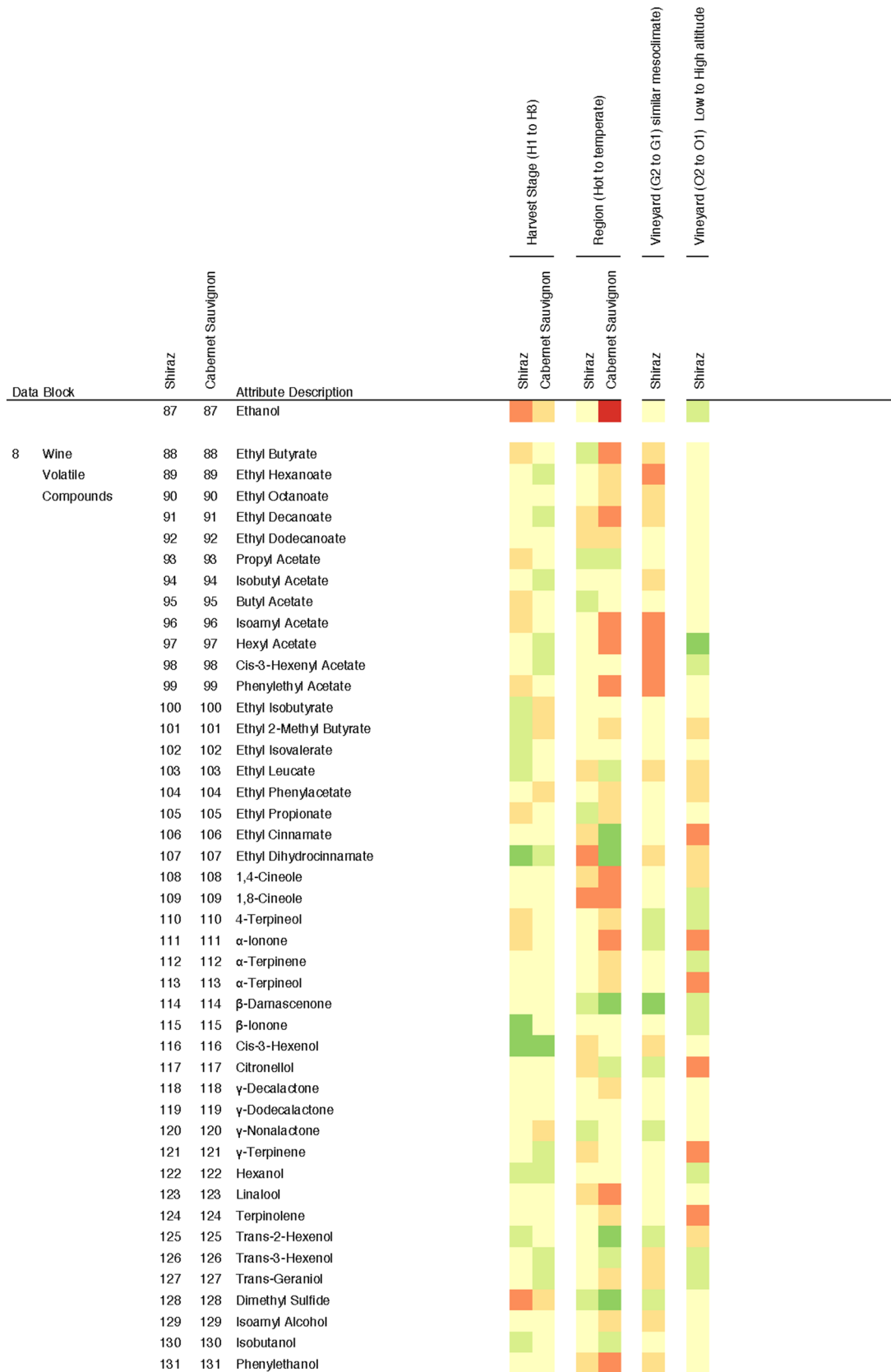


Fig. 2 (continued)

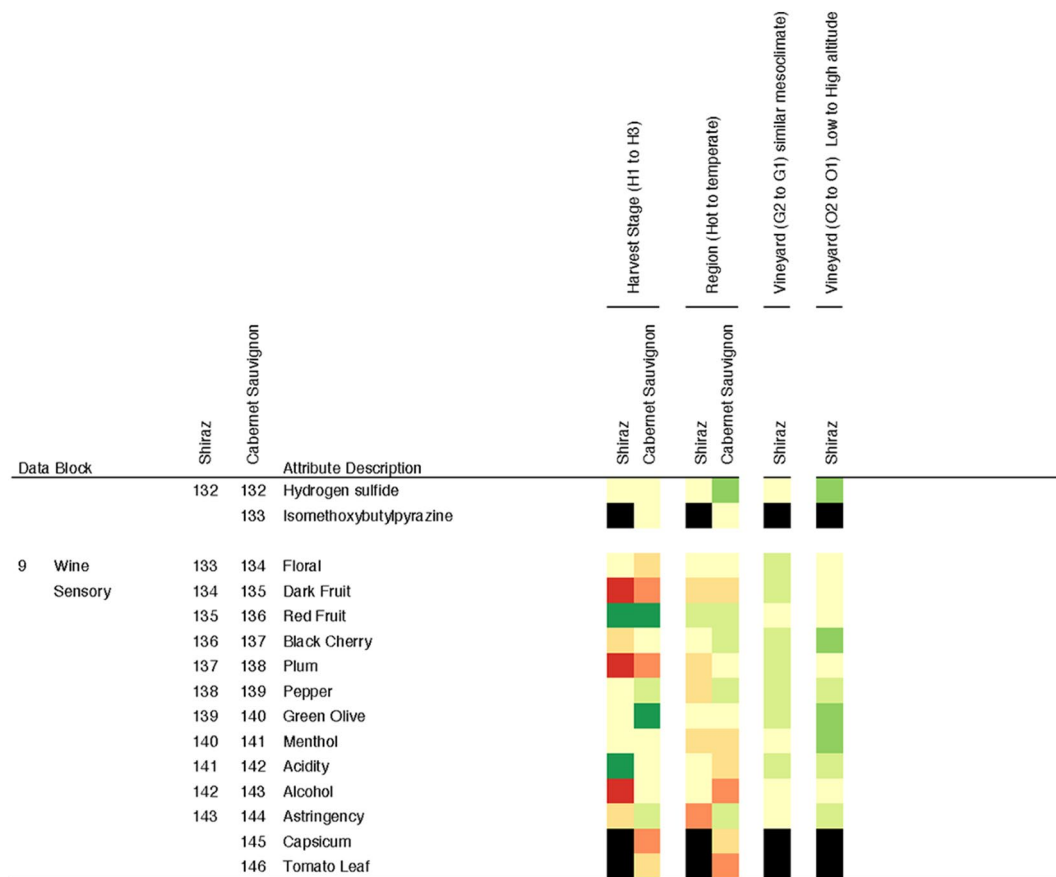


Fig. 2 (continued)

flow. Late season dehydration is common in many varieties, particularly Shiraz in hot and dry years, causing yield reductions up to 25%, and wines with higher alcohols, loss of fresh fruity aromas and pronounced dried fruit character (Chou et al. 2018). An increase in wine glycerol is consistent with higher fermentable carbohydrate levels in grapes as glycerol is expressed as an osmoprotectant by *Saccharomyces cerevisiae* in the early stages of fermentation (Scanes et al. 1998). Wine volatile composition for both cultivars is of interest in that there is little commonality in attribute flux as harvest stages progresses from H1 to H3 which has been reported by this group (Antalick et al. 2015). As expected, malic acid decreased during ripening whereas tartaric acid remained constant.

Grape berry anthocyanins (block 3) were not a significant contributor to sample groupings according to harvest date and low anthocyanin flux is evident in the EF *Harvest*, with grape anthocyanins reaching a maximum at H1 for both Shiraz and Cabernet Sauvignon. This observation is consistent with reports that anthocyanins increase during ripening until approximately 4 to 5 weeks post veraison (Coombe and McCarthy 2000), i.e. before H1. There is no clear link to increasing berry colour and berry maturity

when positioning berry maturing on a sugar accumulation curve. However, berry colour and vineyard are related as evident by the block saliences for site and region for both Shiraz and Cabernet Sauvignon models. Such observations suggests that the composition of anthocyanins in grape berries and thus wine colour potential is intrinsically linked to the vineyard climatic conditions and the practice of delaying grape harvest to attain a specified grape and wine colour may be of limited value.

Grape berry carotenoids decreased with latter harvest dates in both Shiraz in Cabernet Sauvignon. Carotenoids are reduced during ripening via oxidation, thermal and photo—degradation pathways, yielding volatile norisoprenoids or precursors (Mendes-Pinto 2009). Other results of interest for Shiraz included the observations that (E)-hexenol, hexanol and heptanol increased during ripening, whereas (Z)-3-hexenal and trans-geranyl acetone decreased. The volatiles in Cabernet Sauvignon grapes appear to be less influenced by ripening, with only (Z)-3-hexenol, (E)-2-hexenol decreased from H1 to H2. Winemaking parameters are largely indicative of processing attributes and corrective interventions to ensure consistent fermentation profiles were maintained during the investigation.

4.2.2 Site and region

Separate groupings of samples according to site are evident for EF *Region* (Fig. 1 model B and I) and *Site* (Fig. 1 models C, D and J) models having similar block salience values indicating that as vineyard region shifts from a warm (Griffith) to temperate (Orange) climate larger changes in composition occurs in wine chemistry (block 7), wine volatiles (block 8), grape amino acids (block 1), and grape anthocyanins (block 3). A similar picture emerges for EF *Site* (Fig. 1 model J) in the Cabernet Sauvignon models and is consistent with change in mesoclimate associated with lower vineyard temperatures commensurate with higher altitude vineyard locations. Grape amino acids (block 1) and wine volatiles (block 8) are largely impacted as the vineyard mesoclimate (warm to temperate: low to high altitude) changes, and investigations have demonstrated links between berry amino acid and wine ester composition following fermentation (Antalick et al. 2015). Changes to wine ester composition in this investigation are illustrated in the heat map data (Fig. 2; Supplementary Figs. 4 and 5) with most esters in the Cabernet Sauvignon wines increasing in concentration with vineyard mesoclimate moving from warm to temperate. It is somewhat surprising however that wine sensory scores (block 9) were not more highly rated for contribution to sample groupings for *Region*. These observations suggest that wine esters may only contribute a minor role in Cabernet Sauvignon sensory profiles for the wines from this investigation. The importance of methoxypyrazines and high correlations in grapes in cool climate in varietal Cabernet Sauvignon aroma is well understood (Allen and Lacey 1993) and potential interactions between esters and other chemical classes of volatile compounds is deserving of further investigation.

Comparisons of the G2 to G1 (Fig. 1 model D) site locations for the Shiraz vineyards is of interest as these two sites are relatively close and within a region where an unchanging topography creates almost identical meso-climates. Both vineyards were managed with a sprawling canopy and have identical row/vine spacing. Thus some inferences can be made regarding the influence of vineyard management parameters and clonal factors to the variable flux by reference to the heat map summary (Fig. 2). Sites G1 and G2 principally vary in clonal composition and yield per vine. Vineyard parameters such as primary shoots and bunches per vine along with average bunch weight (Supplementary Table 2) will obviously influence the yield per vine. A more detailed investigation of clonal influence with a temporal investigation of yield effect, including a consideration of vine water status, is necessary to fully elucidate the impact of these combined factors on berry and subsequent wine composition. However, it would seem likely that many of the observed differences in the ANOVA model loadings for *Site* in the Shiraz models are influenced by clonal variations

rather than yield. This observation is supported by the large differences observed in the attribute loadings for explanatory factors *Yield* and *Site* presented in the heat map for all significant explanatory factors.

5 Conclusion

Comprehensive targeted metabolite profiling of Shiraz and Cabernet Sauvignon grapes and wines combined with wine making inputs and wine sensory assessments were used to model the flux of compounds that influence wine style and which respond to factors associated with terroir mesoclimate, vineyard site and region. Using a multifactorial experimental design including metabolic and sensory profiles and a multiblock data analysis strategy, consistent trends in wine compositional profiles are evident and can be mapped to grape maturity at harvest for both cultivars, when vineyards were managed to accommodate excessive heat and avoid water stress, irrespective of vineyard location or climate. Insights to aspects of terroir and the major role of mesoclimate, site and grapevine cultivar are demonstrated and provide better understanding of the role for wine production targeting specific wine styles.

Author contributions LS, GA, KS, JWB and AD designed the study, collected samples and performed analysis. JWB conducted sensory studies. LS and JB performed statistical analysis of data. All authors wrote and approved the manuscript.

Funding This study was funded by Australia's grapegrowers and winemakers through their investment body Wine Australia, with matching funds from the Australian Government (Grant NWG1301). The National Wine and Grape Industry Centre is an alliance between Charles Sturt University, New South Wales Department of Primary Industries and the New South Wales Wine Industry Association.

Data availability All data from this study is available from the Charles Sturt University Research Output <https://doi.org/10.26189/5da7a9823c55d>

Compliance with ethical standards

Conflict of interest All authors declare that they have no conflict of interest directly or indirectly related to the research presented in this manuscript.

Ethical approval The study was approved by the Charles Sturt University Faculty of Science Low Risk Ethics Review Committee.

Research involving human participants and/or animals All procedures performed were in accordance with the ethical standards of the institution and/or national research committee and with the 1964 Helsinki declaration and its later amendments or comparable ethical standards.

Informed consent Written informed consent was obtained from every subject before inclusion in this study.

References

- Allen, M. S., & Lacey, M. J. (1993). Methoxypyrazine grape flavor: Influence of climate, cultivar and viticulture. *Wein Wissenschaft*, *48*, 211–213.
- Anesi, A., Stocchero, M., Dal Santo, S., Commisso, M., Zenoni, S., Ceoldo, S., et al. (2015). Towards a scientific interpretation of the terroir concept: Plasticity of the grape berry metabolome. *BMC Plant Biology*, *15*, 191.
- Antalick, G., Perello, M.-C., & de Revel, G. (2010). Development, validation and application of a specific method for the quantitative determination of wine esters by headspace-solid-phase microextraction-gas chromatography–mass spectrometry. *Food Chemistry*, *121*, 1236–1245.
- Antalick, G., Šuklje, K., Blackman, J. W., Meeks, C., Deloire, A., & Schmidtke, L. M. (2015). Influence of grape composition on red wine ester profile: Comparison between cabernet sauvignon and shiraz cultivars from Australian warm climate. *Journal of Agricultural and Food Chemistry*, *63*, 4664–4672.
- Blackman, J., & Saliba, A. (2009). Sensory characterization of hunter valley semillon using descriptive analysis. *Flavour and Fragrance Journal*, *24*, 238–244.
- Boccard, J., & Rudaz, S. (2016). Exploring omics data from designed experiments using analysis of variance multiblock orthogonal partial least squares. *Analytica Chimica Acta*, *920*, 18–28.
- Bouveresse, D. J.-R., Pinto, R. C., Schmidtke, L. M., Locquet, N., & Rutledge, D. N. (2011). Identification of significant factors by an extension of ANOVA-PCA based on multiblock analysis. *Chemometrics and Intelligent Laboratory Systems*, *106*, 173–182.
- Carbonneau, A., Deloire, A., Torregrosa, L., Jaillard, B., Pellegrino, A., Méta, A., et al. (2015). *Traité de la vigne : Physiologie, terroir, culture*. Paris: Dunod.
- Charters, S., Spielmann, N., & Babin, B. J. (2017). The nature and value of terroir products. *European Journal of Marketing*, *51*, 748–771.
- Chou, H.-C., Šuklje, K., Antalick, G., Schmidtke, L. M., & Blackman, J. W. (2018). Late-season shiraz berry dehydration that alters composition and sensory traits of wine. *Journal of Agricultural and Food Chemistry*, *66*, 7750–7757.
- Coombe, B. G., & McCarthy, M. G. (2000). Dynamics of grape berry growth and physiology of ripening. *Australian Journal of Grape and Wine Research*, *6*, 131–135.
- Cramer, G. R., Ghan, R., Schlauch, K. A., Tillett, R. L., Heymann, H., Ferrarini, A., et al. (2014). Transcriptomic analysis of the late stages of grapevine (*Vitis vinifera* cv. Cabernet Sauvignon) berry ripening reveals significant induction of ethylene signaling and flavor pathways in the skin. *BMC Plant Biology*, *14*, 370.
- Deloire, A. (2013). Physiological Indicators to Predict Harvest Date and Wine Style in Beames, K.S., Robinson, E.M.C., Godden, P.W. and Johnson, D.L. (Eds), *15th Australian Wine Industry Technical Conference: Sydney, New South Wales 13–18 July 2013*, The Australian Wine Industry Technical Conference Inc., pp. 47–50.
- Deloire, A., Prévost, P., & Kelly, M. (2008). Unravelling the terroir mystique—an agro-socioeconomic perspective. *Perspectives in Agriculture, Veterinary Science, Nutrition and Natural Resources*, *3*, 1–9.
- Downey, M. O., & Rochfort, S. (2008). Simultaneous separation by reversed-phase high-performance liquid chromatography and mass spectral identification of anthocyanins and flavonols in Shiraz grape skin. *Journal of Chromatography A*, *1201*, 43–47.
- Eyégghé-Bickong, H. A., Alexandersson, E. O., Gouws, L. M., Young, P. R., & Vivier, M. A. (2012). Optimisation of an HPLC method for the simultaneous quantification of the major sugars and organic acids in grapevine berries. *Journal of Chromatography B*, *885–886*, 43–49.
- Frayne, R. F. (1986). Direct analysis of the major organic components in grape must and wine using high performance liquid chromatography. *American Journal of Enology and Viticulture*, *37*, 281–287.
- Gika, H. G., Theodoridis, G. A., Vrhovsek, U., & Mattivi, F. (2012). Quantitative profiling of polar primary metabolites using hydrophilic interaction ultrahigh performance liquid chromatography–tandem mass spectrometry. *Journal of Chromatography A*, *1259*, 121–127.
- Gladstones, J. S. (2011). *Wine, terroir and climate change*. Kent Town, South Australia: Wakefield Press.
- Harrington, P. D. B., Vieira, N. E., Espinoza, J., Nien, J. K., Romero, R., & Yergey, A. L. (2005). Analysis of variance-principal component analysis: A soft tool for proteomic discovery. *Analytica Chimica Acta*, *544*, 118–127.
- Haynes, P. A., Sheumack, D., Greig, L. G., Kibby, J., & Redmond, J. W. (1991). Applications of automated amino acid analysis using 9-fluorenylmethyl chloroformate. *Journal of Chromatography A*, *588*, 107–114.
- Hochberg, U., Batushansky, A., Degu, A., Rachmilevitch, S., & Fait, A. (2015). Metabolic and physiological responses of shiraz and cabernet sauvignon (*Vitis vinifera* L.) to near optimal temperatures of 25 and 35 °C. *International Journal of Molecular Sciences*, *16*, 24276–24294.
- Iland, P., Bruer, N., Edwards, G., Weeks, S., & Wilkes, E. (2004). *Chemical analysis of grapes and wine: Techniques and concepts*. Campbelltown: Patrick Iland Wine Promotions Pty Ltd.
- Jansen, J. J., Hoefsloot, H. C. J., Greef, J. V. D., Timmerman, M. E., Westerhuis, J. A., & Smilde, A. K. (2005). ASCA: analysis of multivariate data obtained from an experimental design. *Journal of Chemometrics*, *19*, 469–481.
- Lashbrooke, J. G., Young, P. R., Strever, A. E., Stander, C., & Vivier, M. A. (2010). The development of a method for the extraction of carotenoids and chlorophylls from grapevine leaves and berries for HPLC profiling. *Australian Journal of Grape and Wine Research*, *16*, 349–360. <https://doi.org/10.1111/j.1755-0238.2010.00097.x>.
- Loscos, N., Hernández-Orte, P., Cacho, J., & Ferreira, V. (2009). Comparison of the suitability of different hydrolytic strategies to predict aroma potential of different grape varieties. *Journal of Agricultural and Food Chemistry*, *57*, 2468–2480.
- Matarese, F., Cuzzola, A., Scalabrelli, G., & D’Onofrio, C. (2014). Expression of terpene synthase genes associated with the formation of volatiles in different organs of *Vitis vinifera*. *Phytochemistry*, *105*, 12–24.
- Matthews, M. A. (2015). *Terroir and other myths of winegrowing*. Oakland, California: University of California Press.
- Mendes-Pinto, M. M. (2009). Carotenoid breakdown products the–norisoprenoids–in wine aroma. *Archives of Biochemistry and Biophysics*, *483*, 236–245.
- Rantalainen, M., Bylesjö, M., Cloarec, O., Nicholson, J. K., Holmes, E., & Trygg, J. (2007). Kernel-based orthogonal projections to latent structures (K-OPLS). *Journal of Chemometrics*, *21*, 376–385.
- Roullier-Gall, C., Lucio, M., Noret, L., Schmitt-Kopplin, P., & Gougeon, R. D. (2014). How subtle is the “Terroir” effect? Chemistry-related signatures of two “Climats de Bourgogne”. *PLoS ONE*, *9*, e97615.
- Santo, S. D., Zenoni, S., Sandri, M., Lorenzis, G. D., Magris, G., Paoli, E. D., et al. (2018). Grapevine field experiments reveal the contribution of genotype, the influence of environment and the effect of their interaction (G×E) on the berry transcriptome. *The Plant Journal*, *93*, 1143–1159.
- Sarneckis, C. J., Damberg, R. G., Jones, P., Mercurio, M., Herderich, M. J., & Smith, P. A. (2006). Quantification of condensed tannins by precipitation with methyl cellulose: development and validation of an optimised tool for grape and wine analysis. *Australian Journal of Grape and Wine Research*, *12*, 39–49.

- Scanes, K. T., Hohmann, S., & Prior, B. A. (1998). Glycerol production by the yeast *Saccharomyces cerevisiae* and its relevance to wine: a review. *South African Journal of Enology and Viticulture*, *19*, 17–24.
- Schmidtke, L. M., Blackman, J. W., Clark, A. C., & Grant-Preece, P. (2013). Wine metabolomics: Objective Measures of sensory properties of semillon from GC-MS profiles. *Journal of Agricultural and Food Chemistry*, *61*, 11957–11967.
- Seguin, G. (1986). 'Terroirs' and pedology of wine growing. *Experientia*, *42*, 861–873.
- Shahood, R., Savoi, S., Bigard, A., Torregrosa, L. and Romieu, C. (2019) From average to individual berry, a paradigm shift for accurate analysis of water and primary metabolites accumulation into grapevine fruit. In *Proceedings of the 21st International Symposium GiESCO* (pp. 354–358).
- Šuklje, K., Carlin, S., Stanstrup, J., Antalick, G., Blackman, J. W., Meeks, C., et al. (2019). Unravelling wine volatile evolution during Shiraz grape ripening by untargeted HS-SPME-GC × GC-TOFMS. *Food Chemistry*, *277*, 753–765.
- Šuklje, K., Zhang, X., Antalick, G., Clark, A. C., Deloire, A., & Schmidtke, L. M. (2016). Berry shriveling significantly alters shiraz (*Vitis vinifera* L.) grape and wine chemical composition. *Journal of Agricultural and Food Chemistry*, *64*, 870–880.
- Tonietto, J., & Carbonneau, A. (2004). A multicriteria climatic classification system for grape-growing regions worldwide. *Agricultural and Forest Meteorology*, *124*, 81–97.
- Wehrens, R., Carvalho, E., Masuro, D., de Juan, A., & Martens, S. (2013). High-throughput carotenoid profiling using multivariate curve resolution. *Analytical and Bioanalytical Chemistry*, *405*, 5075–5086.
- Young, P. R., Eyéghé-Bickong, H. A., du Plessis, K., Alexandersson, E., Jacobson, D. A., Coetzee, Z., et al. (2016). Grapevine plasticity in response to an altered microclimate: Sauvignon blanc modulates specific metabolites in response to increased berry exposure. *Plant Physiology*, *170*, 1235.

Publisher's Note Springer Nature remains neutral with regard to jurisdictional claims in published maps and institutional affiliations.